Perception-Based Data Reduction and Transmission of Haptic Data in Telepresence and Teleaction Systems

Peter Hinterseer, *Member, IEEE*, Sandra Hirche, *Member, IEEE*, Subhasis Chaudhuri, *Senior Member, IEEE*, Eckehard Steinbach, *Member, IEEE*, and Martin Buss, *Member, IEEE*

***Abstract*—We present a novel approach for the transmission of haptic data in telepresence and teleaction systems. The goal of this work is to reduce the packet rate between an operator and a teleoperator without impairing the immersiveness of the system. Our approach exploits the properties of human haptic perception and is, more specifically, based on the concept of just noticeable differences. In our scheme, updates of the haptic amplitude values are signaled across the network only if the change of a haptic stimulus is detectable by the human operator. We investigate haptic data communication for a 1 degree-of-freedom (DoF) and a 3 DoF teleaction system. Our experimental results show that the presented approach is able to reduce the packet rate between the operator and teleoperator by up to 90% of the original rate without affecting the performance of the system.**

***Index Terms*—Compression, deadband, haptics, psychophysics, teleaction, telepresence.**

I. Introduction

TELEPRESENCE AND TELEACTION (TPTA) systems have been and still are the subject of extensive interdisciplinary research covering the areas of communications, computer science, robotics, system theory, and psychology. TPTA systems allow the operator to be present and active in remote environments that can be distant, scaled to macro- or nanoworlds, or hazardous for the human using multiple human sensing modalities. Example applications are telemaintenance, telesurgery, and tele-edutainment.

Manuscript received March 23, 2006; revised May 3, 2007. The associate editor coordinating the review of this manuscript and approving it for publication was Dr. Manuel Davy. This work was supported by the Collaborative Research Center SFB 453 of the German Research Foundation (DFG). The work of S. Chaudhuri was supported by the Alexander von Humboldt Foundation. Part of this work was presented at the ICASSP'05, ICCE'06, Haptics Symposium'06, and ICASSP'06.

P. Hinterseer and E. Steinbach are with the Institute of Communication Networks (LKN), Media Technology Group, Technische Universitaet Muenchen, 80290 Muenchen, Germany (e-mail: ph@tum.de; eckehard.steinbach@tum.de).

S. Hirche is with the Fujita Laboratory, Department of Mechanical and Control Engineering, Tokyo Institute of Technology, Tokyo 152-8552, Japan (e-mail: hirche@lsr.ei.tum.de).

S. Chaudhuri is with the Department of Electrical Engineering, Indian Institute of Technology, Bombay, Powai, Mumbai 400 076, India (e-mail: sc@ee.iitb.ac.in).

M. Buss is with the Institute of Automatic Control Engineering, Technische Universitaet Muenchen, 80290 Muenchen, Germany (e-mail: mb@tum.de).

Color versions of one or more of the figures in this paper are available online at http://ieeexplore.ieee.org.

Digital Object Identifier 10.1109/TSP.2007.906746

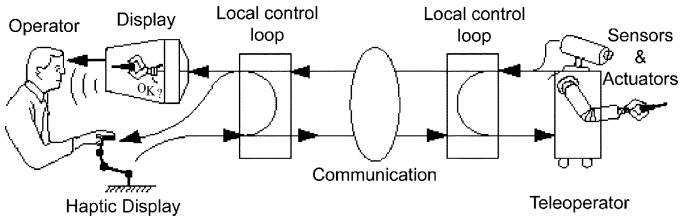

Fig. 1. General overview of a TPTA system (adapted from [5]).

A TPTA system, visualized in Fig. 1, consists of three main components: the human system interface (HSI), the teleoperator, and the communication link connecting them. The HSI acts both as the data input (typically haptic devices for position/orientation input) and data output device (HMD for stereo-video, headphones for audio, and again, the haptic devices for force/torque feedback). By means of the HSI the operator (OP) commands the position/velocity of the teleoperator (TOP) while he observes the remote scene through multimodal feedback. The teleoperator is a robot equipped with multiple sensors (video-camera, microphones, and force/torque sensors) and actuators to interact with the remote environment, e.g., an object. The multimodal sensor data including the environment interaction force is fed back to the HSI and displayed to the operator. The communication link transports the multimodal data streams bidirectionally. Ideally, the operator feels as if he was in place of the robot interacting with the environment, i.e., is completely immersed. The main focus in this article is on the haptic (force feedback) system, specifically on the data reduction and transmission of haptic data streams within a TPTA system.

Haptic data like position, velocity, and force are sampled by the corresponding sensors at the HSI and TOP at a constant rate, typically in the range 500–1000 Hz with a resolution of 16 bit per DoF. The high sampling rate is necessary to ensure the tracking performance and stability of the local control loops at the HSI and the TOP. Currently available TPTA systems may easily have more than 20 DoFs (bimanual systems with additional finger force feedback). At every sampling instant a data packet consisting of all current sample values is generated and sent out. The bidirectionally transmitted position/velocity and force data packets serve as reference input for the local control loops at HSI and TOP. A global control loop is closed over the communication system. It is evident that the communication introduces transmission time delay in this control loop. It is well known that time delay in a closed loop system leads to instability if not treated by appropriate control measures [6]. The higher the time delay the more conservative the control has to be designed

in order to guarantee stability. This on the other hand leads to a strong deterioration of immersiveness, and very likely to the inoperability of the TPTA system [7]–[12]. Thus, hard realtime constraints apply for the haptic data stream, and this is the fundamental difference to standard streaming multimedia such as video and audio. The primary design goal for a communication system for TPTA systems is to keep the introduced delays and the amount of data being sent as small as possible.

The primary purpose of this paper is to investigate psychophysical data reduction methods for haptic data streams. For efficient transmission of haptic data over the Internet, data reduction techniques have to be used to lower the amount of data and in our case the rate at which packets have to be transmitted. Reduced packet rates put less demand on the Internet connection and therefore lower the probability of congestion along the transmission path. High packet rates (1000 Hz) as we can observe them for traditional transmission of haptic data are hard to maintain over the Internet [13]. Traditional block-based compression techniques are not applicable because of the additional delay introduced by building blocks of data. Stream-based techniques like differential coding followed by entropy coding (e.g., [12]) work quite well with up to 90% packet payload reduction but suffer from a bad packet header to payload ratio. For instance, if a haptic data stream carries 3-DoF data with 16 bit resolution the payload of one packet is 6 byte. In comparison, the UDP/IP header of this packet is 28 byte. Along with the negative effects of differential coding like vulnerability to packet loss this approach is not suitable for packet-based communication in TPTA systems.

Surprisingly, compression of haptic data has not been a field of intensive research so far. With recent advances in virtual reality (VR), telerobotics, and telepresence and teleaction, however, the topic is rapidly gaining relevance. Once haptic data has to be transmitted or stored an interest in compressing this kind of data emerges. Reference [14] presents a first overview of possible methods for haptic data compression mostly for storage applications where [12], [15], [16] go further into detail and present schemes using DPCM, ADPCM, and Huffman Coding. In [17] compression based on predictive coding is applied in order to improve the communication between a haptic device and the controlling host with respect to sampling rate and data rate. All the mentioned approaches have in common that they only exploit statistical signal properties for data reduction. In comparison, the approach presented in this work exploits the characteristics of human haptic perception in order to reduce the packet transmission rate in networked TPTA systems. To the best of our knowledge, this is the first psychophysics-based haptic data reduction approach in the literature.

II. Psychophysical Background

The transmission approach presented in this work is based on the exploitation of limitations of human haptic perception. The basic principle is that events a human being cannot perceive are not transmitted over the network. Human perception has been investigated intensively during the past two centuries. In this context, the respective perceptual threshold values for all kinds of stimuli put on the human body have been studied. Apart from very detailed information for every modality a human being can perceive, one major conclusion emerged from these studies:

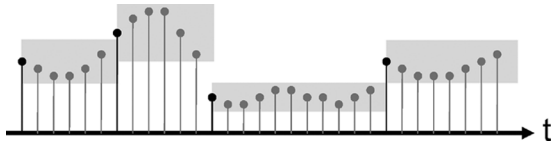

Fig. 2. 1-DoF deadband applied to a signal. Gray samples are not sent. Black samples are signalled to the receiver.

Human haptic perception can be well approximated by Weber's Law. Ernst Weber was an experimental physiologist who, in 1834, first discovered the linear relationship

$$\frac{\Delta I}{I} = k \quad \text{or} \quad \Delta I = kI \tag{1}$$

between the stimulus intensity I and the smallest still perceivable change of the stimulus intensity ΔI. The constant k is in modern psychophysics literature referred to as Weber constant or just noticeable difference (JND) (in older literature ΔI has been called JND) or differential threshold. The JND is measured in psychophysical experiments and represents a statistical rather than an exact quantity. The JND usually reported is the difference that a person notices on 50% of the trials.

For haptic perception, i.e., force, limb position, and velocity, the JND is in the range from 5% to 15%, depending on the type of stimulus and the limb/joint where it is applied [18], [19]. This means that if, for example, the displayed force at the HSI changes its magnitude by less than the JND, the operator would not notice this change.

III. Data Reduction for Haptic Communication

A. Deadband Principle

The basic idea of the psychophysically motivated data reduction approach presented in this paper is to transmit data only if the operator is likely to detect the change compared to previously transmitted data. Related schemes are the deadband approach applied in networked control systems [20] where signal changes are not transmitted unless they exceed a certain fixed threshold and the well-known Δ-modulation ([21], [22]). In our approach, the threshold is magnitude-dependent. The deadband that is formed by applying this threshold value with respect to the most recently transmitted magnitude value will be called p in the following. p is a percentual value. The deadband principle as we apply it here is illustrated in Fig. 2. The parameter k in Weber's Law (1) basically states the upper bound of the deadband p. If, for example, the user is presented with a force of 1 N and the deadband is given with $p = 10\%$ the next force sample value is only transmitted once it goes either below 0.9 N or above 1.1 N. Every force change in the interval from 0.9 to 1.1 N is considered imperceptible by the human operator and therefore not necessary to be transmitted. Once p is larger than k the deviation between the transmitted and original signal is likely to become perceivable to the user and interaction may feel distorted and the quality of immersion is reduced.

To apply the deadband algorithm, the magnitude of the difference d between an initial value v_i and a current value v_c has to be computed. This is done by calculating the absolute difference between those two sample values and comparing it to a

threshold value (the deadband p multiplied by the initial value v_i).

$$\begin{aligned} & d = |v_i - v_c| \\ & d \leq |p \cdot v_i| \quad \Longrightarrow \quad \text{Do nothing} \\ & d > |p \cdot v_i| \quad \Longrightarrow \quad \text{Transmit new value } v_c. \end{aligned} \tag{2}$$

As the control loops at the HSI and the TOP require an input signal at a constant high sampling rate, samples which are not transmitted have to be reconstructed at the receiver side. It is straightforward to apply a zero-order-hold strategy, where the value of the most recently received sample is held until a new sample arrives.

Note that every data reduction in a closed loop system has an influence on the system dynamics, and as such possibly on the stability. Stability under lossy data reduction, as well as effects of additional communication time delay have been investigated in other works of the authors [23], [24], and will not be treated here. Furthermore, we will consider a position/velocity-force architecture here, where the position/velocity is transmitted from the HSI to the TOP and the force from the TOP to the HSI. The velocity, as well as the force, is processed using the deadband approach. In order to prevent a drift between the positions of the HSI and the TOP resulting from the lossy nature of the data reduction algorithm, additionally a position update is sent with every velocity packet.

B. Limitations of a 1-DoF Deadband Approach

In TPTA applications, we often encounter haptic devices with multiple degrees of freedom, often 3. A 3-DoF device typically uses the three Cartesian components (or another representation of 3-D space) of the current velocity or force. Applying the 1-DoF deadband approach to every single component of the Cartesian representation is a straightforward extension, which, however, turns out to be very inefficient with respect to the data transmission rate.

If random movements with identically distributed directions and magnitudes of forces and velocities are examined, the component with the lowest magnitude and therefore the smallest deadband is mostly responsible for packet generation. The probability of having a component with low magnitude therefore increases with the number of components used. It becomes obvious that the more DoFs a system has, the less efficient the deadband transmission approach becomes if separately applied to each DoF.

C. Extension to Multiple DoFs

To overcome the aforementioned limitation, we propose a multidimensional deadband approach. This approach is motivated by recent psychophysical results [25] indicating the valididty of the straightforward extension of Weber's Law to n dimensions. In the following we explain the extension of the one-dimensional (1–D) deadband [a numeric interval, see (2)] to two dimensions where the deadband becomes a circular area. In 3-D, a spherical volume element serves as deadzone (we will denote a multidimensional deadband as deadzone from now on) and the extension is similar to the 2–D case.

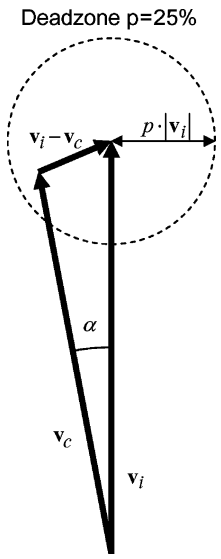

Fig. 3. Geometrical description of a 2-DoF deadzone.

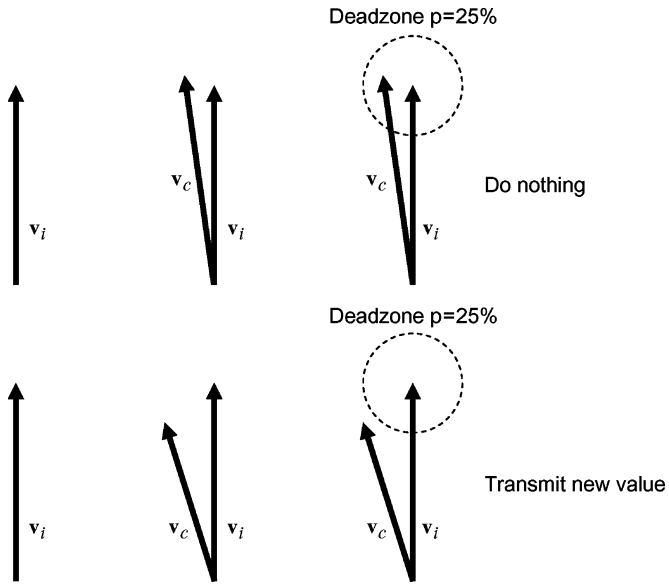

Fig. 4. Criterion for transmission of new values in the 2-DoF case.

From now on, vector values are considered and are denoted in bold letters $\mathbf{v}_i$ and $\mathbf{v}_c$, and d represents the magnitude of their difference. Accordingly, the deadzone algorithm reads as follows:

$$\begin{aligned} & d = |\mathbf{v}_i - \mathbf{v}_c| \\ & d \leq p \cdot |\mathbf{v}_i| \quad \Longrightarrow \quad \text{Do nothing} \\ & d > p \cdot |\mathbf{v}_i| \quad \Longrightarrow \quad \text{Transmit new vector } \mathbf{v}_c. \end{aligned} \tag{3}$$

Fig. 3 illustrates the resulting deadzone. The deadzone is represented by a circle around the tip of vector $\mathbf{v}_i$ with radius $p \cdot |\mathbf{v}_i|$. The angle between $\mathbf{v}_i$ and $\mathbf{v}_c$ is denoted by α. The multi-DoF deadband principle is visualized in Fig. 4. If the tip of vector $\mathbf{v}_c$ lies within the deadzone circle, the deadband is not violated and thus no new value is transmitted. If the tip lies outside the deadzone circle, updated sample values are sent.

The circular shape of the deadzone makes it computationally easy to calculate whether the deadzone is violated or not. The size of the deadzone circle depends only on the length of vector $\mathbf{v}_i$ whereas the maximum of the angle α depends only on the deadband factor p.

The angle α reaches its maximum, when

$$\mathbf{v}_c \perp \mathbf{v}_i - \mathbf{v}_c \tag{4}$$

and

$$|\mathbf{v}_i - \mathbf{v}_c| = p \cdot |\mathbf{v}_i| \tag{5}$$

i.e., $\mathbf{v}_c$ is tangential to the deadzone circle. p is assumed to be significantly smaller than 1. So α_{max} can be calculated as follows:

$$\sin \alpha_{max} = \frac{|\mathbf{v}_i - \mathbf{v}_c|}{|\mathbf{v}_i|} = \frac{p \cdot |\mathbf{v}_i|}{|\mathbf{v}_i|} = p \tag{6}$$

$$\alpha_{max} = \arcsin p. \tag{7}$$

In this case $|\mathbf{v}_{c_{\alpha max}}|$ would be

$$\begin{aligned} \cos \alpha_{\max} &= \frac{|\mathbf{v}_{c_{\alpha max}}|}{|\mathbf{v}_i|} \\ |\mathbf{v}_{c_{\alpha max}}| &= \cos \alpha_{max} \cdot |\mathbf{v}_i| \\ &= \cos(\arcsin p) \cdot |\mathbf{v}_i|. \end{aligned} \tag{8}$$

This means that no matter how large a sampled 2-DoF variable (velocity, force, ...) is, once it changes its direction by α_{max} an updated value will be sent to the receiver. The multidimensional deadband algorithm hence provides a magnitude independent deadband as far as direction is concerned. This is an important property of the isotropic deadzone.

The extension of this approach to 3-D is straight forward. The vectors $\mathbf{v}_i$ and $\mathbf{v}_c$ become 3-D, the circular deadzone becomes a spherical deadzone. The tip of $\mathbf{v}_c$ has to lie outside this sphere to trigger an update value. The values of $\alpha_{\max}$ and $|\mathbf{v}_{c\alpha max}|$ stay the same, because the vectors $\mathbf{v}_i$ and $\mathbf{v}_c$ define a plane in which the above calculations hold.

D. Model-Based Prediction

In order to further reduce the amount of transmitted packets, signal prediction is used on both sides of the system as shown in Fig. 5. On the OP side a force predictor is used to estimate future force values from the incoming force values. On the TOP side the same predictor is fed with the values sent to the OP side. The fact that the predictors on OP and TOP side are strictly coherent (neglecting the unavoidable delay between the models because of transmission delays) enables us to only send packets over the network if the current actual signal differs from the predicted signal by the deadband/deadzone. A similar prediction is performed for the velocity values which are transmitted in the opposite direction.

As an example of such a real time signal prediction a relatively simple linear predictor is implemented and experimentally analyzed in this paper

$$v_i = \begin{cases} v_{\text{new}} & \text{value sent/arrived} \\ v_{i-1} + \frac{v_{\text{new}-1} - v_{\text{new}-2}}{t_{\text{new}-1} - t_{\text{new}-2}} (t_i - t_{i-1}) & \text{else} \end{cases} \tag{9}$$

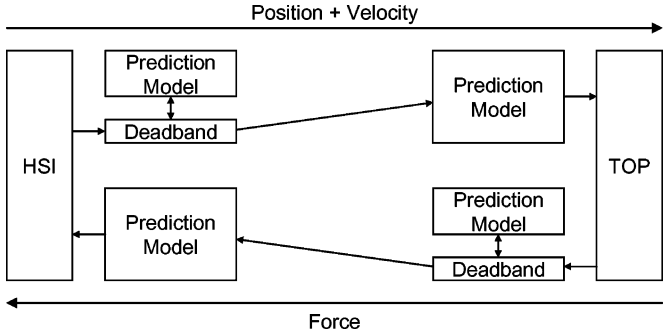

Fig. 5. System with model-based prediction for higher packet rate reduction.

where $\{v_i, v_{i-1}, v_{i-2}, \ldots\}$ are the most current values output by the model and $\{t_i, t_{i-1}, t_{i-2}, \ldots\}$ are the corresponding time instances. $\{v_{\text{new}}, v_{\text{new}-1}, v_{\text{new}-2}, \ldots\}$ and $\{t_{\text{new}}, t_{\text{new}-1}, t_{\text{new}-2}, \ldots\}$ are the last sent/received values and the corresponding time instances.

With this predictor the signal is estimated by following the slope given by the last two received signal values. Once the predicted signal differs too much from the actual signal, a new correct value is transmitted and the new prediction starts from there. More specifically, if the actual value falls outside the psychophysically motivated deadband around the predicted value we consider the prediction error to be noticeable and correct it by sending the actual value.

The control loops which secure the safe operation of both OP and TOP are normally updated at a fixed sampling rate. Having a prediction model as shown above enables us to use almost arbitrary sampling rates for those control loops. A strict match between OP and TOP sampling rates is no longer necessary, because the prediction model can be evaluated at any sampling rate and is updated as soon as it differs from the desired values.

E. Practical Implementation Issues

Polynomial extrapolation, here a first-order extrapolation, is known to be sensitive to high-frequency disturbances. Any high frequency sensor noise on the input signal results in large prediction errors and as a result in an unnecessary high utilization of the communication link. In real TPTA systems, especially the velocity signal is very noisy as it is not measured directly but derived from a discrete time difference approximation of the measured quantized position signal. Noise naturally also occurs in force measuring but does not have the spiky behavior of the velocity signal. Therefore, the input to the predictor is lowpass filtered with a cut-off frequency beyond the perception range. This cut-off frequency depends on a number of factors. One being the modality the filter is used on. For example, force noise can be detected to much higher frequencies than velocity noise. Another is that the display device has limitations for position/force display with respect to displayable frequencies. In our case the cut-off frequency was determined experimentally.

IV. Experimental Verification

Several experiments have been conducted in order to verify the proposed data reduction techniques. A 1-DoF experiment is used to determine the detection threshold of the deadband parameter p and to relate it to the JND k. In the 3-DoF experiments the user utility of the proposed 3-DoF approaches is determined.

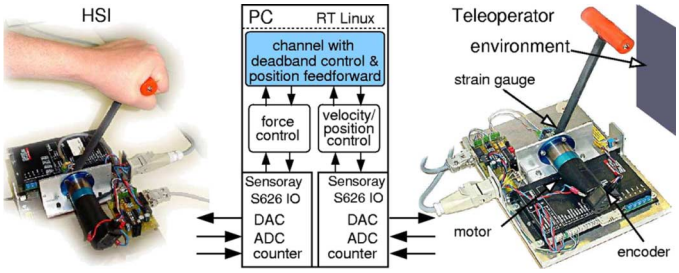

Fig. 6. Experimental setup with two 1-DoF haptic devices.

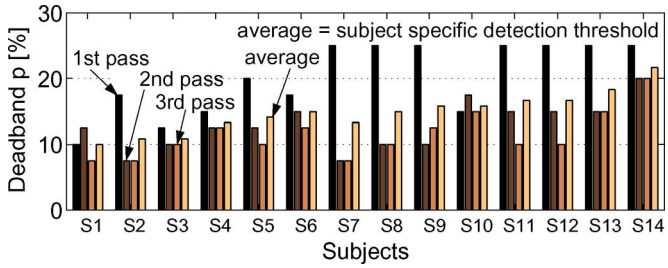

Fig. 7. Subject-specific detection thresholds for p in the 1-DoF experiment.

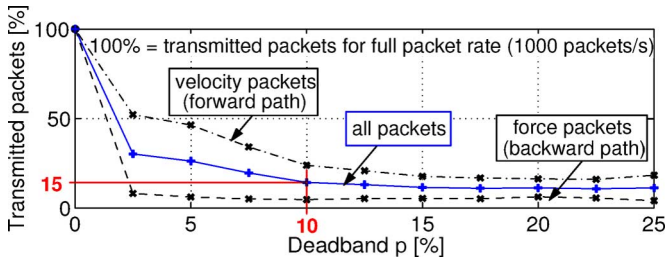

Fig. 8. Influence of the deadband width on the packet rate: Average number of transmitted packets (percentual packet rate) as a function of the deadband parameter p.

A. *1-DoF Approach*

Our design goal is to minimize the network traffic while maintaining immersiveness as indicated in the previous sections. As a first step psychophysical experiments were conducted for the 1-DoF case in order to determine the maximum value of the deadband parameter p where a degradation of the immersiveness is not perceivable. Furthermore, the effect on the network traffic is studied.

1) Setup: The experimental setup consists of two identical 1-DoF haptic displays connected to a PC and a stiff wall as the environment (see Fig. 6). The angle is measured by an incremental encoder, the force by a strain gauge. The sensor data is processed in the PC where all control algorithms including the deadband algorithm are implemented. The velocity/position is transmitted to the TOP acting as the set value for the local control loop of the TOP. The TOP tracks the movement of the HSI and communicates the measured contact force back to the HSI as the set value for the force control loop.

2) Procedure: Altogether 14 subjects (3 female, 11 male, aged 20–50) were tested for their detection threshold of the deadband parameter p. The subjects sat in front of the HSI lever and were told to operate it with their preferred hand. They were equipped with earphones to mask the sound the device motors generate. During a familiarization phase the subjects were told to feel the hard contact, a stiff wall by which the lever movement was restricted at the TOP side, through the system at a sampling rate of 1000 Hz and without any deadband transmission algorithm applied. As soon as they felt familiar with the system the measurement phase began. The deadband parameter detection thresholds were determined using a three interval forced choice (3IFC) paradigm. The subjects were presented with three consecutive 20 s intervals in which they should operate the system. Only in one of the three intervals, which was randomly selected, the deadband algorithm with a certain value p was applied. The other two were without deadband control. Every three intervals the subject had to tell which of the intervals felt different from the other two. The experiment started with a deadband parameter $p = 2.5\%$ and was increased after every incorrect answer up to a maximum of 25%. When an answer was correct, the same value was used again until three consecutive right answers were given. After this first pass, the subjects were told how the distortion feels like and with what kind of technique they should be able to perceive it best. Then the same procedure as before was applied (second pass). After another three consecutive right answers p was reduced by 50% without telling the subjects and the procedure was repeated in order to verify the detection threshold one more time (3rd pass). The mean value of the three p values at which the consecutive right answers occurred were taken as the deadband detection threshold for the specific subject.

3) Results: The specific results for every subject are shown in Fig. 7. Comparing the results of the three passes for the individual subject, all subjects had a significantly higher detection threshold in the first pass when they did not know what kind of distortion they had to expect. Hence, the distortion introduced by this deadband approach is not necessarily perceived as disturbing or impairing the contact impression. The subject specific detection thresholds are in the range between 10% and 22.5%. Only one subject managed to detect the distortion introduced by $p = 10\%$. For the remaining 13 subjects corresponding to 93% a higher threshold was determined. Eleven subjects (79%) had a detection threshold $p > 11\%$. The measured detection thresholds are in the range of the JNDs reported for velocity and force perception [18], [19]. It should be noted, however, that JND's are typically determined in static conditions. Here a temporal change of the signal is considered. The relation between the JNDs obtained by psychophysical experiments for static conditions and our deadband results for dynamic manipulation conditions needs further investigation.

In order to investigate the effect of deadband control on the packet rate, the induced network traffic was recorded during the experimental user study. The mean percentage of transmitted packets as a function of the deadband parameter p is shown in Fig. 8. 100% represent the standard approach with 1000 packets/s on the forward and the backward path, respectively. As expected, higher deadband parameters lead to higher traffic reduction. The traffic volume induced by velocity packets is already at 25% at a deadband size of $p = 10\%$ and keeps falling with increasing deadband size. The impact on the number of force packets transmitted is even higher. Already at $p = 2.5\%$ the network traffic volume in the backward path is less than 10% of the standard approach. At $p = 10\%$ only 15% of the original number of packets is transmitted. This means an

Fig. 9. The SensAble Phantom Omni device used for the experiments [http://www.sensable.com].

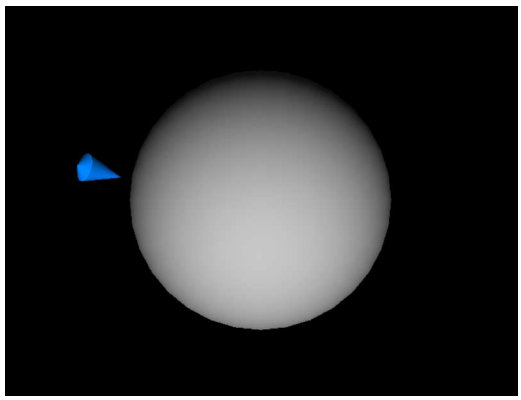

Fig. 10. The graphical display of the OP side (HSI).

average network traffic reduction by 85%. Ninety–three percent of the subjects were not able to feel the distortion introduced by the corresponding deadband parameter.

B. 3-DoF Approaches

In order to verify the presented 3-DoF deadzone approaches (3-DoF alone, 3-DoF with model based prediction, and 3-DoF with model based prediction and filtering), several experiments with a commercially available 3-DoF haptic device were conducted. In difference to the previous experiment, not a single detection threshold is determined, but the quality of immersiveness is rated over a range of deadband values as a first step towards a user utility function. The influence of the deadband is further investigated separately for the force and the velocity data.

The conducted experiment for the 3-DoF approaches was a haptic interaction task with a remote virtual environment. The hardware and software setup is the following: On the OP side the haptic display device SensAble PHANTOM Omni (see Fig. 9) serves as the HSI. Over a 100 Mbit/s Ethernet LAN connection this OP side transmits current position and velocity samples to a simulated haptic environment on another machine in the same LAN.

1) Setup of OP Side:

a) Haptic display device: The haptic device is capable of 6-DoF input and 3-DoF output. This means that both the endeffector's position in space as well as its orientation can be read from the device drivers. In contrast to that it is only possible to output forces in 3-DoFs namely the three directions in space. The torques necessary for altering the endeffector's orientation cannot be produced. In our experiment, the additional 3-DoFs of endeffector orientation are only used to display the 3-D-cursor of the graphical display correctly. They are neither sent to the TOP side nor do they have any other influence.

b) Graphical display: The graphical display consists of an OpenGL-based 3-D visualization of the workspace. Both the current cursor position and the position of the haptically manipulated object are displayed. See Fig. 10 for an impression of the HSI graphical display.

What one sees in this display is a gray sphere in the middle of the workspace of the haptic display device along with the blue cursor which signifies the current position and orientation of the device.

The pose of the haptic display device is sampled at 1000 Hz. The graphical display is refreshed with the standard refresh rate of 60 Hz.

c) Deadzone implementation: The three components of the current device velocity are combined in a 3-D vector. According to the formulas in Section III-C the size of the deadzone is calculated. The reference (or initial) vector is always the one which was last transmitted to the receiver. Every 1 ms a new value of the 3-D velocity vector is read from the device drivers and it is decided whether its tip lies in the deadzone or not. According to the result of the decision, a new vector is sent to the receiver or the new vector is discarded.

d) Position update: The sending of only velocity values in such a deadband system would result in a more or less severe degradation of position tracking. It is, therefore, necessary to send the actual position values along with the current velocity values so that the TOP can take care of position errors. Since the packet sizes are very small this additional amount of data is negligible. The packet rate is not increased.

2) Setup of TOP Side:

a) Virtual environment: The virtual environment is implemented by a C++-Class which manages the positions and properties of virtual objects which are to be manipulated as well as the positions of one or more users interacting with the environment. It is capable of 3-DoF input and 3-DoF output. This means it is fed with a 3-DoF velocity input (along with a 3-DoF position input for reasons of position tracking) and calculates the resulting forces for this position. The environment as well as the haptic display device at the OP side are refreshed at a rate of 1000 Hz. Unlike the systems in [26] and [27] which also implement a virtual haptic environment it is intentional that all computations concerning the haptic feedback are done centralized on one machine like in [28]. This central approach is chosen in order to have a system which is as comparable as possible to a real TPTA system. Also unlike to [29] where only one packet is in transit at all times for stability reasons, the presented system communicates in both directions at the same time. Stability problems were not observed.

b) Sphere object: The only object in the virtual environment in this experiment is a sphere in the middle of the virtual workspace. This sphere is registered with the sphere in the graphical display (see Section IV-B-1-b) so that contacts between the cursor and the sphere in the graphical display exactly correspond with contacts in the virtual environment. The virtual sphere is fixed at the center of the workspace and can be touched with the virtual cursor. The resulting force during the interaction is calculated by Hooke's Law

$$F = u \cdot b \tag{10}$$

where u is the stiffness of the sphere and b the amount of penetration into the sphere body. F is the resulting force magnitude. The direction of the force always points from the sphere center to the actual cursor position. It is calculated as

$$\mathbf{F} = \frac{\mathbf{x} - \mathbf{s}}{|\mathbf{x} - \mathbf{s}|} \cdot (r - |\mathbf{x} - \mathbf{s}|) \cdot u \tag{11}$$

where the resulting force vector $\mathbf{F}$ is determined from the current position of the user $\mathbf{x}$, the sphere position in space $\mathbf{s}$, the sphere radius r, and the stiffness u.

c) Deadzone implementation: The initial vector for the deadzone calculation is the force vector which was last sent to the OP side. Every time the virtual haptic model is updated it either sets the most current position and velocity values for the user position (in case an update packet has arrived) or calculates a new position from the last known user position, the last known user velocity, and the exact time since the last update. This updated position is then used to calculate an updated force which then is used as the current vector for the deadzone calculations. In case the deadzone is violated by the new vector, a new packet containing the updated force vector is sent and the sent vector serves as the new initial vector.

3) Subjective Evaluation: Ten test subjects underwent the experimental procedure described in the following to determine suitable values for the deadband parameters so that no degradation of immersiveness can be noticed.

The following cases were considered:

- Deadzone on velocity values only (3-DoF) as described in Section III-C
- Deadzone on force values only (3-DoF) as described in Section III-C
- Deadzone on velocity with linear prediction (3-DoF LP) as described in Section III-D
- Deadzone on force with linear prediction (3-DoF LP) as described in Section III-D
- Deadzone on velocity with linear prediction on filtered data (3-DoF LP + Filter)
- Deadzone on force with linear prediction on filtered data (3-DoF LP + Filter)

The subjects are first presented with a system without deadband to get used to handling the device and to experience what it feels like. Then a heavily distorted system is shown to the subjects in which they can clearly feel the kind of distortion which is introduced into the system by the deadzone algorithm. This phase is called the familiarization phase.

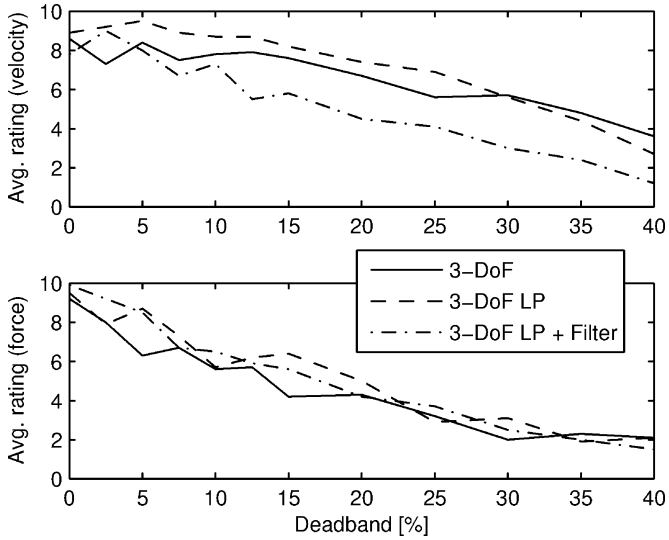

Fig. 11. User ratings for the deadband presentations in the 3-DoF approaches.

After the subjects feel familiar with the system and they know the kind of distortion they are presented with, two test runs are conducted each consisting of twelve 30 s intervals (24 intervals in 12 min total) in which the subjects were told to haptically explore the virtual environment and to assess the quality of the haptic presentation. In the first run with twelve intervals the deadband is only used for the velocity values which are sent from the OP to the TOP. In the second run, the deadband is only used on force values which are sent from the TOP to the OP. During the tests, the subjects wore headphones so they could concentrate on their haptic sensations.

In the 12 intervals of each run, we apply a randomly chosen order of the following possible deadband values: 0%, 2.5%, 5%, 7.5%, 10%, 12.5%, 15%, 20%, 25%, 30%, 35%, and 40%. The subjects do not know either which value was currently used or in which communication direction the deadband was applied.

After every interval the subject is required to rate the presentation. If it felt exactly like the undistorted signal from the familiarization phase, they should give a rating of 10 points. If it felt just as bad as the heavily distorted signal from the familiarization phase, they should give a rating of 1 point. The ratings in between can be chosen according to the quality of the signal where higher ratings signify better quality.

4) Results and Discussion: The results for the mentioned 3-DoF approaches can be seen in Figs. 11 and 12.

a) 3-DoF without prediction and filtering: The results are represented by the solid lines in Figs. 11 and 12.

From Fig. 11 it can be observed that a deadzone usage on velocity values seems to be far less perceptible than on force values. One can see that the velocity deadband can be increased to up to 20% while still reaching an average rating of almost 7 points, which most subjects described as barely perceivable distortion. In comparison, the force deadband should not be far above 5% for the average rating to also stay above seven points.

This behavior has two reasons. The first reason lies in the fact that the used TOP is a VR environment. Position errors can be corrected by just setting the actually transmitted position

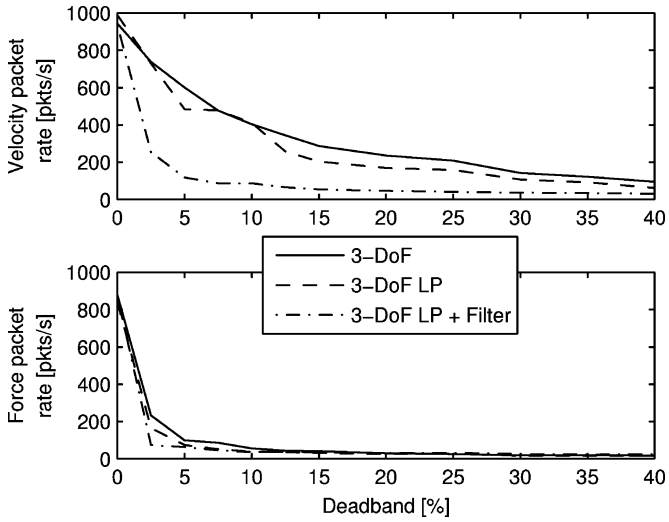

Fig. 12. Resulting packet rates of the 3-DoF approaches.

value as the current position. In a real TPTA system it is more difficult to correct this position error because the endeffector has to be moved towards the correct position. This introduces additional distortion whereas in VR environments the position can be updated instantaneously.

The second reason lies in the deadband principle itself. As we have mentioned in Section III-A, a new value is only transmitted if the user can sense the introduced change. This is of course true for the direction from the TOP to the OP. The transmitted forces are directly sensed by the human being. In contrast to this in the other direction no human sensory system is involved. So there is basically no reason to transmit new velocity values adapted to human perception. Velocity updates are processed by a nonhuman system which uses it merely to generate new force values for the HSI. Therefore environment dynamics have an influence on the possible degree of deadband application. Consequently we can see that it is often possible (at least in the presented case, which stands somehow for most VR haptic environments) to use deadband transmission far beyond human haptic sensory capabilities for the direction from OP to TOP.

With respect to the resulting packet rates the first observation is that, in general, more velocity packets than force packets are generated as can be seen in Fig. 12. This also has multiple reasons. First, velocity packets have to be sent all the time for tracking the endeffector whereas force packets have only to be sent when contact with the environment takes place. Second, force usually reaches higher magnitudes (and therefore higher deadbands) more quickly than velocities. In the case of this experiment, the test subjects are in contact with the environment almost all the time, and so velocity is mostly small whereas force is quite high in most cases. The third reason lies in the differentiation of already noisy position values in order to get the desired velocity signal. This differentiation amplifies the noise and this high amount of noise is therefore another reason for triggering the deadband, especially when it is small in magnitude.

It can be observed that with 0% deadband less than 1000 packets per second are sent. This comes from the fact that even with 0% deadband a change in the measured variable must occur to trigger a new packet transmission. In the case of calculated forces of the VR environment, force is exactly zero while no contact to the environment is made. Therefore only in case of contact packets are sent. Knowing that, we can conclude that during the experiments with 0% deadband the subjects had contact with the environment about 87% of the time.

In comparison to our results for the 1-DoF case in Section IV-A-3, we can conclude that the deadband usage in three dimensions leads to similar tendencies in packet rate reduction as the 1-DoF approach but is not quite as effective as such. Packet rates for velocity packets are reduced by almost 75% when using a barely perceivable 20% deadband. For force packets a reduction by almost 90% is possible by chosing the also barely perceivable 5% deadband.

b) 3-DoF with linear prediction: The dashed lines in Figs. 11 and 12 show the corresponding results.

The ratings in Fig. 11 given by the test subjects are almost always above those of the previously mentioned case. Hence it is possible to use even larger deadbands when prediction is applied.

We can see that even the simple linear prediction model in Section III-D reduces the packet rates in comparison to the 3-DoF approach in the previous paragraph. In Fig. 12, we observe for a 20% velocity deadband and a 5% force deadband an improvent of 28% and 25%, respectively. The total savings in comparison to transmission without deadband are 83% and 93% for velocity and force packets, respectively.

One possibility to further improve this approach is to use more sophisticated prediction methods. However, the limiting factor is signal noise as the following experiment shows.

c) 3-DoF with linear prediction and filtered input signals: The results are represented by the dash-dotted lines in Figs. 11 and 12.

In Fig. 11 we can see an almost linear decrease in the ratings for both types of data with increasing deadband value. We assume that values of 7 and higher represent a good feeling of immersion in the system. Consequently, we can say that 10% deadband for both velocity and force should not be exceeded so as not to sacrifice immersion.

With respect to packet rates, compared to the results from the previous paragraph where no pre-filtering was applied, we can observe a drastic decrease in velocity packet rates, especially for small deadband values. This is exactly the benefit the prefiltering was supposed to give. This has two main reasons. First, during motion phases with small velocities the velocity noise triggered unnecessary packet transmissions. With reduced noise in the signal this happens considerably less often. Second, less noise makes it easier to estimate and predict signal slopes.

For force packet rates the improvements are not as significant as in the velocity case. The reason for this is the fact that we have considerably lower noise levels on the force signal to begin with. The prefiltering step is, therefore, not as efficient here as for velocity signals. Still we can observe a significant improvement (55%) in packet rate at 2.5% deadband in comparison to the LP case. This means almost 93% packet rate reduction in comparison to the original rate with only a minimal 2.5% deadband applied.

Finally, we can state that the proposed pre-filtering step for prediction based deadband transmission of 3-D haptic data works well for velocity and force data. At a combination of 7.5% deadband for velocity and 2.5% deadband for force we achieve a reduction of packet rate to 8.7% of the original rate for velocity and 7.4% for force with barely noticeable influence on immersiveness.

d) Discussion: It is very likely that the presented results can be transferred to more complex scenarios and tasks. The operation of more complex or more dynamic scenes should not be very different. The results from [18], [19] are for static conditions. However, all our results point in the direction that thresholds similar to the static JND are valid for the dynamic case. To the best of our knowledge, research in psychophysics has not yet considered spatiotemporal behavior of the JND in literature. We will investigate this issue in our future work.

Perceptual thresholds in combination with the resulting packet rates allow us to choose optimal trade offs. For force samples it is generally not necessary to choose thresholds higher than a few percent because packet rates are already very low at this point. For velocity it is highly dependent on the amount of noise in the signal, but generally we can say that 10% to 20% should be possible in most cases.

With increasing system complexity in terms of the number of DoFs used for interaction, the approaches become less efficient. This is because only three directional or angular DoFs can be combined in a reasonable way. If more DoFs are used, they have to be grouped and every group may trigger a packet transmission at every sampling instant. Finding reasonable combinations of more than 3 DoFs in the case that data generation is synchronized over these DoFs is subject to future research.

V. Conclusion

The transmission of haptic data is a relatively new challenge in multimedia communication. In this paper, methods are presented which exploit the properties of human haptic perception for data reduction of haptic data. The basic deadband approach is presented together with its extensions to 3-DoF and further enhancements using linear prediction and filtering. Those techniques which are presented in this work are to our knowledge the first psychophysically motivated data reduction approaches for haptic data in literature. The usage of those in modern telepresence and teleaction systems makes it possible to use the Internet as the communication infrastructure. This forms the base for easier access and simpler realization of haptics-based applications.

References

[1] P. Hinterseer, E. Steinbach, S. Hirche, and M. Buss, "A novel, psychophysically motivated transmission approach for haptic data streams in telepresence and teleaction systems," in *Proc. IEEE Int. Conf. Acoust., Speech, Signal Process.*, Philadelphia, PA, Mar. 2005, pp. 1097–1100.

[2] P. Hinterseer, E. Steinbach, and S. Chaudhuri, "Model based data compression for 3D virtual haptic teleinteraction," in *Proc. IEEE Int. Conf. Consum. Electron.*, Las Vegas, NV, USA, Jan. 2006, pp. 23–24.

[3] P. Hinterseer and E. Steinbach, "A psychophysically motivated compression approach for 3D haptic data," in *Proc. IEEE Haptics Symp.*, Alexandria, VA, Mar. 2006, pp. 35–41.

[4] P. Hinterseer, E. Steinbach, and S. Chaudhuri, "Perception-based compression of haptic data streams using kalman filters," in *Proc. IEEE Int. Conf. Acoust., Speech, Signal Process.*, Toulouse, France, May 2006.

[5] W. R. Ferrell and T. B. Sheridan, "Supervisory control of remote manipulation," *IEEE Spectrum*, vol. 4, no. 10, pp. 81–88, 1967.

[6] R. Anderson and M. Spong, "Bilateral control of teleoperators with time delay," *IEEE Trans. Autom. Control*, vol. 34, pp. 494–501, 1989.

[7] S. Hirche, A. Bauer, and M. Buss, "Transparency of haptic telepresence systems with constant time delay," in *Proc. IEEE Int. Conf. Control Appl.*, Toronto, Canada, 2005, pp. 328–333.

[8] S. Hirche, *Haptic Telepresence in Packet Switched Communication Networks*, ser. Nr.1082 in Fortschrittsberichte VDI, series 8: Mess-, Steuerungs- und Regelungstechnik. Düsseldorf, Germany: VDI-Verlag, 2005, Ph.D. dissertation.

[9] K. S. Park and V. Kenyon, "Effects of network characteristics on human performance in a collaborative virtual environment," in *Proc. IEEE Virtual Reality Conf.*, Houston, TX, Aug. 1999, pp. 104–111.

[10] E. Ou and C. Basdogan, "Network considerations for a dynamic shared haptic environment," in *Proc. Nat. Conf. Undergrad. Res.* , Whitewater, WI, Apr. 2002.

[11] R. T. Souayed, D. Gaiti, G. Pujolle, W. Yu, Q. Gu, and A. Marshall, "Haptic virtual environment performance over IP networks: A case study," in *IEEE Symp. Distrib. Simul. Real-Time Appl.*, Delft, Netherlands, Oct. 2003, pp. 181–189.

[12] A. Kron, G. Schmidt, B. Petzold, M. F. Zäh, P. Hinterseer, and E. Steinbach, "Disposal of explosive ordnances by use of a bimanual haptic telepresence system," in *Proc. IEEE Int. Conf. Robot. Autom.*, New Orleans, LA, Apr. 2004, pp. 1968–1973.

[13] C. Mahlo, C. Hoene, A. Rosami, and A. Wolisz, "Adaptive coding and packet rates for TCP-friendly voip flows," in *Proc. 3rd Int. Symp. Telecommun.*, Shiraz, Iran, Sep. 2005.

[14] C. Shahabi, A. Ortega, and M. R. Kolahdouzan, "A comparison of different haptic compression techniques," in *Proc. IEEE Int. Conf. Multimed. Expo.*, Lausanne, Switzerland, Aug. 2002, pp. 657–660.

[15] A. Ortega and Y. Liu, "Lossy compression of haptic data," in *Touch in Virtual Environments: Haptics and the Design of Interactive Systems*. Englewood Cliffs, NJ: Prentice-Hall, 2002, ch. 6, pp. 119–136.

[16] K. Hikichi, H. Morino, I. Fukuda, S. Matsumoto, Y. Yasuda, I. Arimoto, M. Iijima, and K. Sezaki, "Architecture of haptics communication system for adaptation to network environments," in *Proc. IEEE Int. Conf. Multimed. Expo.*, Tokyo, Japan, Aug. 2001, pp. 744–747.

[17] C. W. Borst, "Predictive coding for efficient host-device communication in a pneumatic force-feedback display," in *Proc. First Joint Eurohaptics Conf. Symp. Haptic Interfaces for Virtual Environ. Teleoperator Syst.*, Pisa, Italy, Mar. 2005, pp. 596–599.

[18] L. A. Jones and I. W. Hunter, "Human operator perception of mechanical variables and their effects on tracking performance," *Adv. Robot.*, vol. 42, pp. 49–53, 1992.

[19] G. C. Burdea, *Force and Touch Feedback for Virtual Reality*. New York: Wiley, 1996.

[20] P. G. Otanez, J. R. Moyne, and D. M. Tilbury, "Using deadbands to reduce communication in networked control systems," in *Proc. Amer. Control Conf.*, Anchorage, AK, May 2002.

[21] H. R. Schindler, "Delta modulation," *IEEE Spectrum*, vol. 7, pp. 69–78, 1970.

[22] J. A. Greefkes and K. Riemens, "Code modulation with digitally controlled companding for speech transmission," *Philips Tech. Rev.*, vol. 31, pp. 335–353, 1970.

[23] S. Hirche, P. Hinterseer, E. Steinbach, and M. Buss, "Towards deadband control in networked teleoperation systems," in *Proc. IFAC World Congress, Int. Federation of Autom. Control*, Prague, Czech Republic, 2005.

[24] S. Hirche, P. Hinterseer, E. Steinbach, and M. Buss, "Network traffic reduction in haptic telepresence systems by deadband control," in *Proc. IFAC World Congress, Int. Federation of Autom. Control*, Prague, Czech Republic, 2005.

[25] J. Drösler, "An n-dimensional Weber law and the corresponding Fechner law," *J. Math. Psychol.*, vol. 44, pp. 330–335, 2000.

[26] J. P. Hespanha, M. McLaughlin, and G. S. Sukhatme, "Haptic collaboration over the internet," in *Touch in Virtual Environments: Haptics and the Design of Interactive Systems*. Englewood Cliffs , NJ: Prentice-Hall, 2002, ch. 8, pp. 158–168.

[27] Y. Ishibashi, T. Hasegawa, and S. Tasaka, "Group synchronization control for haptic media in networked virtual environments," in *Proc. 12th Int. Symp. Haptic Interfaces for Virtual Environ. Teleoper. Syst.*, Chicago, IL, Mar. 2004, pp. 106–113.

[28] H. R. Choi, B. H. Choi, and S. M. Ryew, "Haptic display in the virtual collaborative workspace shared by multiple users," in *Proc. 6th IEEE Int. Workshop on Robot and Human Commun.*, Sendai, Japan, Sep. 1977, pp. 478–483.

[29] I. Elhajj, N. Xi, W. K. Fung, Y. H. Liu, W. J. Li, T. Kaga, and T. Fukuda, "Haptic information in internet-based teleoperation," *IEEE/ASME Trans. Mechatronics*, vol. 6, no. 3, pp. 295–304, Sep. 2001.

Peter Hinterseer (M'04) was born in Germany in 1976. He received the diploma in electrical engineering in 2002 from the Technische Universität München, Munich, Germany.

He is currently working toward the Ph.D. degree with the Media Technology Group, Institute of Communication Networks, Technische Universität München. His research interests include the compression and transmission of multimodal data in telepresence and teleaction systems.

Sandra Hirche (M'07) was born in Germany in 1974. She received the diploma engineering degree in mechanical engineering and transport systems in 2002 from the Technical University Berlin, Germany, and the Doctor of Engineering degree in electrical engineering and computer science in 2005 from the Technische Universität München, Munich, Germany.

Since 2005, she has been a Japanese Society for the Promotion of Science (JSPS) PostDoc with the Tokyo Institute of Technology, Tokyo, Japan. Her research interests include control over communication networks, networked control systems, cooperative control, human-machine interaction, mechatronics, multimodal telepresence systems, and perception-oriented control.

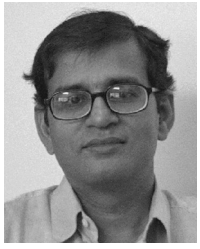

Subhasis Chaudhuri (SM'02) was born in Bahutali, India. He received the B.Tech. degree in electronics and electrical communication engineering from the Indian Institute of Technology (IIT), Kharagpur, in 1985. He received the M.S. and the Ph.D. degrees, both in electrical engineering, from the University of Calgary, Calgary, Canada, and the University of California, San Diego, respectively.

He joined the IIT, Bombay, in 1990 as an Assistant Professor and is currently serving as a Professor and the Head of the department. He has also held visiting positions with the University of Erlangen-Nuremberg, Technical University of Munich, Germany, and the University of Paris XI, France. His research interests include image processing, computer vision, and multimedia. He is a coauthor of the books *Depth From Defocus: A Real Aperture Imaging Approach* and *Motion-Free Super-Resolution* (New York: Springer, 1999). He has also edited a book *Super-Resolution Imaging* (Boston, MA: Kluwer Academic, 2001).

Dr. Chaudhuri is a Fellow of the Alexander von Humboldt Foundation, Germany, the Indian National Academy of Engineering, and the National Academy of Sciences, India. He is the recipient of the Dr. Vikram Sarabhai Research Award for the year 2001, and the Swarnajayanti Fellowship in 2003. He received the S.S. Bhatnagar Prize in engineering sciences for the year 2004. He was a Program Co-Chair for ICCV 2005 Conference held in Beijing, China.

Eckehard Steinbach (M'96) studied electrical engineering at the University of Karlsruhe, Karlsruhe, Germany, the University of Essex, Colchester, U.K., and ESIEE, Paris, France. He received the Engineering Doctorate from the University of Erlangen-Nuremberg, Germany, in 1999.

From 1994 to 2000, he was a Member of the Research Staff of the Image Communication Group, University of Erlangen-Nuremberg. From February 2000 to December 2001, he was a Postdoctoral Fellow with the Information Systems Lab, Stanford University, Stanford, CA. In February 2002, he joined the Department of Electrical Engineering and Information Technology, Technische Universität München, Munich, Germany, as a Professor for Media Technology. His current research interests are in the area of audio-visual-haptic information processing, image and video compression, error-resilient video communication, and networked multimedia systems.

Martin Buss (M'95) was born in Germany in 1965. He received the diploma engineer degree in electrical engineering in 1990 from the Technical University Darmstadt, Germany, and the Doctor of Engineering degree in electrical engineering from the University of Tokyo, Tokyo, Japan, in 1994. In 2000, he finished the habilitation with the Department of Electrical Engineering and Information Technology, Technische Universität München, Munich, Germany.

In 1988, he was a research student with the Science University of Tokyo for one year. As a Postdoctoral Researcher, he was with the Department of Systems Engineering, Australian National University, Canberra, during 1994–1995. From 1995 to 2000, he was a Senior Research Assistant and Lecturer with the Department of Electrical Engineering and Information Technology, Institute of Automatic Control Engineering, Technical University Munich. He was appointed Full Professor, Head of the Control Systems Group, and Deputy Director of the Institute of Energy and Automation Technology, Faculty IV—Electrical Engineering and Computer Science, Technical University Berlin, Germany, from 2000 to 2003. Since 2003, he has been a Full Professor (Chair) with the Institute of Automatic Control Engineering, Technische Universität München. His research interests include automatic control, mechatronics, multimodal human-system interfaces, optimization, nonlinear, and hybrid discrete-continuous systems.